

## The calcium binding properties and structure prediction of the Hax-1 protein

Anna Balcerak, Sebastian Rowinski, Lukasz M. Szafron and Ewa A. Grzybowska<sup>✉</sup>

Cancer Center Institute, Warsaw, Poland

**Hax-1 is a protein involved in regulation of different cellular processes, but its properties and exact mechanisms of action remain unknown. In this work, using purified, recombinant Hax-1 and by applying an *in vitro* autoradiography assay we have shown that this protein binds  $Ca^{2+}$ . Additionally, we performed structure prediction analysis which shows that Hax-1 displays definitive structural features, such as two  $\alpha$ -helices, short  $\beta$ -strands and four disordered segments.**

**Key words:** Hax-1, tags removal, calcium binding, 3D protein model

**Received:** 21 February, 2017; **revised:** 19 April, 2017; **accepted:** 07 June, 2017; **available on-line:** 01 September, 2017

<sup>✉</sup>e-mail: [ewag@coi.waw.pl](mailto:ewag@coi.waw.pl)

**Abbreviations:** PONDR, predictor of natural disordered regions; IDPs, intrinsically disordered proteins

### INTRODUCTION

Hax-1, a 35 kDa protein, was originally identified in lymphocytes as a factor interacting with HS-1 (hematopoietic specific protein 1), possibly involved in signal transduction, leading to B-cell proliferation or apoptosis (Suzuki *et al.*, 1997). Its deficiency is associated with severe congenital neutropenia (Klein *et al.*, 2007), while its overexpression has been detected in several tumors (Trebinska *et al.*, 2010). Further studies have revealed antiapoptotic properties of Hax-1 (Chao *et al.*, 2008; Cilenti *et al.*, 2004; Han *et al.*, 2006; Kang *et al.*, 2010), as well as its involvement in regulating cell migration (Radhika *et al.*, 2004; Ramsay *et al.*, 2007) and associations with the cytoskeleton (Gallagher *et al.*, 2000). Hax-1 was also shown to bind mRNA (Al-Maghrebi *et al.*, 2002; Sarnowska *et al.*, 2007), which suggests that it may influence the fate of transcripts, and act as a regulatory protein operating at the posttranscriptional level. Thus, Hax-1 represents a multifunctional factor involved in the regulation of pivotal cellular processes, but its mechanisms of action remain elusive, and no specific molecular function, except for binding to a plethora of factors (proteins and RNA molecules), has been assigned to this protein (Fadeel & Grzybowska, 2009).

It is noteworthy that Hax-1 lacks homology to any known protein. Initially, it was thought to possess homology domains resembling BH domains of the Bcl-2 family of apoptotic regulators (Suzuki *et al.*, 1997), but this finding was demonstrated to be at least debatable (Jeyaraju *et al.*, 2009; Kokoszynska *et al.*, 2010). The only unquestionable features of Hax-1 appear to be: an acidic domain (30–40 aa) exclusively composed of aspartic and glutamic acid residues, and a PEST sequence, which was shown to be a functional degradation signal (Li *et al.*, 2012). The existence of a transmembrane domain at

the C-terminus of the protein was also discussed, but it appears to be smaller than the analogous domain of the Bcl-2 family of proteins (Jeyaraju *et al.*, 2009). Thus, it is arguable if this hydrophobic region can anchor the protein in the mitochondrial or endoplasmic reticulum membranes. Additionally, a previously-made bioinformatic analysis suggested the existence of a potential single EF-hand calcium-binding site in Hax-1 (Kokoszynska *et al.*, 2010). Calcium-binding capabilities of Hax-1 could be crucial for its biological activity, and an *in vitro* verification of these *in silico* results may lead to a breakthrough in the Hax-1 functional studies. To date, Hax-1 has been reported to bind several calcium-regulating proteins, including phospholamban (PLN) and a calcium pump SERCA2, which is important for maintaining calcium homeostasis in the endoplasmic reticulum and also affects calcium-dependent apoptosis (Vafiadaki *et al.*, 2009; Vafiadaki *et al.*, 2007; Trębińska *et al.*, 2014). Additionally, in a recent report (Hirasaka *et al.*, 2016), the C-terminal domain of Hax-1 was shown to undergo a calcium-induced conformational change, which facilitates UCP3-Hax-1 complex formation. In contrast to earlier results (Kokoszynska *et al.*, 2010), the authors have suggested that  $Ca^{2+}$  may bind to the C-terminal region of Hax-1. In order to further analyze Hax-1 properties, it is necessary to obtain Hax-1 in its soluble and untagged form.

Hax-1 overexpression in bacteria is quite challenging, since it may impair growth of some bacterial strains and is often deposited in inclusion bodies. Previously, our group established conditions for purifying a rat recombinant Hax-1 protein (Sarnowska *et al.*, 2007). In this work, His-tagged Hax-1 was fused to thioredoxin to enhance solubility of the protein. Such a big tag could have potentially impaired functional properties of the recombinant Hax-1 protein. Therefore, we developed an optimized procedure, that allows an isolation of untagged Hax-1 protein, thus, making it potentially suitable for functional or structural analyses. Such research is pivotal to explain how Hax-1 functions at the molecular level, since current knowledge on Hax-1 structure and its physical properties is scarce. Herein, we demonstrate calcium-binding properties of the purified protein, which may shed new light on Hax-1 functional studies. Moreover, we present a structure of this protein, which we obtained using an *in silico* analysis.

### MATERIALS AND METHODS

**Plasmid constructs.** Generation of the pET201\_TRX\_Hax-1\_6xHis expression vector containing rat Hax-1 cDNA (variant I) has been previously described (Sarnowska *et al.*, 2007). Here, we modified this vec-

tor in order to group the two tags together and cleave off the pure protein product. This construct was generated in two steps: in the first step, Hax-1 cDNA was amplified, using pET201\_TRX\_Hax-1\_6xHis as a template, with a reverse primer containing the HindIII site (5'-aagcttTCACTATCGGGACCGAAACCAAC-3'), introducing stop codons between Hax-1 and 6xHis-tag (sequence), destroying protein fusion at the C-terminus and a forward primer without modifications, containing BamHI site (5'-CATggatccGAGCGTCTTTG-3'). The PCR product was cloned into pET201\_TRX\_Hax-1\_6xHis cleaved with BamHI and HindIII, replacing the previous rat Hax-1 cDNA clone and generating the construct encoding rat Hax-1 fused to thioredoxin, but without the His-tag (pET201\_TRX\_Hax-1). In the second step, 6xHis-tag was introduced at the N-terminus of the fusion protein, using the 6xHis-tag-encoding forward primer, containing NdeI site (5'-AcatatgCAT-CATCACCATCACCACATGACTAGTGATAAAAT-TATTC-3') and the reverse primer, containing BamHI site (5'-CAACggatccATGCTAGCCTTGT-3') to generate the PCR product. This product was cloned into the pET201\_TRX\_Hax-1 vector, using restriction sites NdeI and BamHI. We named the resulting expression vector pET201\_6xHis\_TRX\_Hax-1. All cloning steps were verified by sequencing.

**Overexpression in bacteria and protein purification using NiNTA resin.** Overexpression in *E. coli* BL21 DE3. The procedure was carried out as described by Sarnowska and coworkers (2007), with modifications. Plasmids pET201\_TRX\_6xHis (encoding only thioredoxin with His tag) and pET201\_6xHis\_TRX\_Hax-1 were freshly transformed for each isolation into the BL21 DE3 *E. coli* strain. 100 ml of LB medium, containing 100 µg/ml ampicillin, and 12.5 µg/ml chloramphenicol was inoculated with 1 ml of the transformation mixture, without plating. After 16 hours of growth in an orbital shaker (37°C, 210 rpm), 3 ml of the overnight culture was used to inoculate each of 300 ml LB supplemented with 100 µg/ml ampicillin and 12.5 µg/ml chloramphenicol. Bacteria were grown at 37°C until the optical density of the culture at 600 nm (OD) was between 0.4–0.6. The bacterial culture was induced with 1mM IPTG and carried out for 2.5 hours. Every 30 minutes, a 0.5 ml sample was removed from the culture to assess the efficiency of induction. Bacterial cultures were harvested by spinning down at 7500×g for 15 min. The medium was aspirated and the pellets were frozen at -70°C for further processing.

**Protein purification.** The experiment was performed according to the Qiaexpressionist handbook instructions (Qiagen), with modifications. Cells were re-suspended in a lysis buffer, modified by the addition of Triton X-100 to enhance protein solubility (50 mM NaH<sub>2</sub>PO<sub>4</sub>·12H<sub>2</sub>O, 300 mM NaCl, 5 mM imidazol, 0.5% Triton X-100, pH 8.0) with lysozyme 1mg/ml (Sigma) and a protease inhibitor cocktail (cComplete™, EDTA-free Protease Inhibitor Cocktail, Roche) and subsequently broken-up by sonication in an ice bath for short pulse of one second followed by three seconds pause for a total sonication time of 16 min. Cell debris was collected by centrifugation (20000×g at 4°C for 45 min) and the supernatant was filtered using a 0.45 µm pore size (Millipore) followed by incubation with 1.5 ml NiNTA resin (Qiagen) that had been pre-equilibrated with the lysis buffer. Binding to resin was conducted for 1 hour at 4°C on a rotary mixer. Afterwards, the resin was washed three times with 8 ml of a Wash Buffer (50 mM NaH<sub>2</sub>PO<sub>4</sub>·12H<sub>2</sub>O, 300 mM NaCl, 20 mM imidazole, pH 8.0) and eluted

with a high concentration of imidazole in the elution buffer (50 mM NaH<sub>2</sub>PO<sub>4</sub>·12H<sub>2</sub>O, 300 mM NaCl, 250 mM imidazol, pH 8.0).

**Enterokinase digestion.** Enterokinase digestion was performed “on beads”, using EnterokinaseMax (EKMax, Invitrogen). During the last steps of protein purification, after the resin had been washed three times with a wash buffer, the beads were subjected to additional 2 washes with 2× beads volume (3 ml) and with the native binding buffer without NaCl (50 mM NaH<sub>2</sub>PO<sub>4</sub>, 10 mM imidazole). After the last wash, 450 µl of the same buffer was supplemented with 50 µl of 10x EKMax™ Reaction Buffer (500 mM Tris-HCl, pH 8.0, 10 mM CaCl<sub>2</sub>, 1% Tween-20) and 10 µl of EKMax™. The resin was settled-down by gravity. Cleavage conditions were as follows: at 4°C, for 12 and 16 hours, and at 37°C, for 12 and 16 hours. The tag-free Hax-1, as the cleaved product, was released from the resin with the digestion buffer.

**Western blot.** Proteins were extracted by incubation with the Laemmli loading buffer at 98°C for 10 min, separated by electrophoresis on a 12% SDS-polyacrylamide gel and electro-transferred onto a PVDF membrane (Millipore). Western-blot analyses were performed using WestPico, (Pierce), according to the manufacturer's instructions. Antibodies used were: mouse anti-HAX1 primary antibody (1:250, BD Biosciences), HRP-conjugated anti-mouse secondary (1:10000, Abcam).

**Ca<sup>2+</sup> binding assay.** The experiments were performed as described by Maruyama and coworkers (1984). Briefly, after SDS-PAGE electrophoresis in 15% polyacrylamide gel, proteins were electroblotted onto nitrocellulose (Millipore, 0.45 µm pore size) and washed three times for 20 min, each in 60 mM KCl, 5 mM MgCl<sub>2</sub>, 10 mM imidazole-HCl (pH 6.8). The membrane was then incubated for 10 min in the same buffer but to which 0.4 mCi/ml (without the carrier) <sup>45</sup>CaCl<sub>2</sub> had been added, washed in H<sub>2</sub>O for 5 min, and air-dried. The <sup>45</sup>CaCl<sub>2</sub> was purchased from Perkin Elmer (Calcium-45 Radionuclide, 10.70 mCi/mg, concentration 17.70 mCi/ml, 655.02 Mbq/ml, Calcium Chloride in Aqueous Solution). Autoradiographs of the <sup>45</sup>Ca<sup>2+</sup>-labeled proteins were obtained by exposure to an Amersham Hyperfilm™ ECL in an Amersham autoradiography cassette, equipped with intensifying screens, for 28 days at -70°C. Proteins bound to nitrocellulose were detected by staining with PonceauS (Sigma). Calmodulin (Sigma), was used as a positive control. The amounts of proteins were calculated using ImageJ software based on PonceauS staining, with reference to the guidelines found at <http://www.di.uq.edu.au/sparqimagejblots>.

**Structure prediction analysis.** Secondary structure prediction was performed using the PredictProtein 2013 (Technical University of Berlin, Germany) (Yachdav *et al.*, 2014) <https://www.predictprotein.org/>. Disordered regions were detected using PONDR (Predictor of Natural Disordered Regions) <http://www.pondr.com/>.

In silico computation of the secondary and tertiary structure of the rat Hax-1 followed by the estimation of its potential biological function, involving predictions of Gene Ontology (GO) and ligand binding sites, were carried out using the I-TASSER meta server, a unified platform for automated protein structure and function predictions (<http://zhanglab.cmb.med.umich.edu/I-TASSER/>) (Roy *et al.*, 2010; Yang *et al.*, 2015, Zhang 2008). The 3-dimensional model of Hax-1 was visualized in the Swiss-PdbViewer and animated with record-MyDesktop and Kdenlive software.

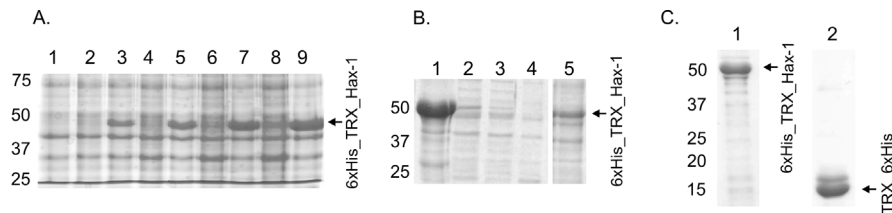


**Figure 1. Hax-1 overexpression and purification on NiNTA resin.**

(A) Induced expression of the recombinant Hax-1 protein (bacterial lysate). Molecular weight marker: Precision Plus Protein Dual Color Standards, lanes: 1. bacterial lysate before induction 2. 0.5 hour without induction-control 3. 0.5 hour after induction with IPTG 4. 1 hour without induction-control 5. 1 hour after induction with IPTG 6. 1.5 hour without induction-control 7. 1.5 hour after induction with IPTG 8. 2.5 hours without induction-control 9. 2.5 hours after induction with IPTG. (B) Protein purification steps; lanes: 1. cell pellet in a urea buffer, 20  $\mu$ l 2. bacterial lysate, 25  $\mu$ l 3. cell supernatant, 25  $\mu$ l 4. wash #1, 25  $\mu$ l 5. elution, 30  $\mu$ l (C) Recombinant Hax-1 and thioredoxin samples compared for equal loading estimation, lanes: 1. Recombinant Hax-1 protein after elution: 10  $\mu$ l, 2. Thioredoxin after elution, not diluted, 10  $\mu$ l.

## RESULTS

### Hax-1 overexpression, purification and tags removal

The pET201\_6xHis\_TRX\_Hax-1 construct (Supplementary Fig. 1 at [www.actabp.pl](http://www.actabp.pl)) was used to transform the BL21 *E. coli* strain. Protein purification was performed on the NiNTA resin under native conditions. The results of induction and elution are presented in Fig. 1A, B. Additionally, thioredoxin with 6xHis-tag was generated using the same procedure and the relative yield of the two proteins was compared for further experiments (Fig. 1C). Hax-1 overexpression in BL21 *E. coli* was followed by incomplete purification, up to three washes, and stopped before elution. The protein at this point was bound to the resin and the impurities were washed off. The next step consisted of on-resin cleavage with a specific enterokinase digestion buffer, under different duration and temperature conditions (Fig. 2A). After cleavage, the tags remained bound to the resin while the cleaved protein was collected in the flow-through fraction (Fig. 2B). Subsequent elution resulted in a mixture of the double-tagged and untagged

Hax-1 protein. The presence of untagged protein in the mixture is addressed in the discussion section.

### Binding of $Ca^{2+}$ by purified Hax-1

The recombinant Hax-1 protein with the thioredoxin tag and the His-tag were used in a calcium-binding assay (Fig. 3A). To eliminate the possibility that the thioredoxin tag bestows calcium-binding properties upon the recombinant protein, a control sample with purified thioredoxin (similar amount as in Hax-1 sample, estimated by Coomassie staining) was measured likewise, showing a slight band, compared to a relatively strong signal obtained for the recombinant Hax-1 protein. However, since the differences were not very pronounced, when estimated by PonceauS staining, the results could not be considered as conclusive. To provide further evidence that untagged Hax-1 can bind  $Ca^{2+}$ , an experiment was carried out using a mixture of the double-tagged and untagged protein, obtained in the eluate after enterokinase cleavage. A mixture of the two proteins from the elution step was used in this experiment, because it contained higher amounts of the untagged Hax-1 protein than the homogenous, untagged protein preparation. The identity of the protein products was determined by Western blotting. Since the two proteins were separated on a polyacrylamide gel and then transferred onto a membrane for an incubation with the  $^{45}Ca^{2+}$  isotope, signals from the tagged and untagged protein can be easily distinguished (Fig. 3B).

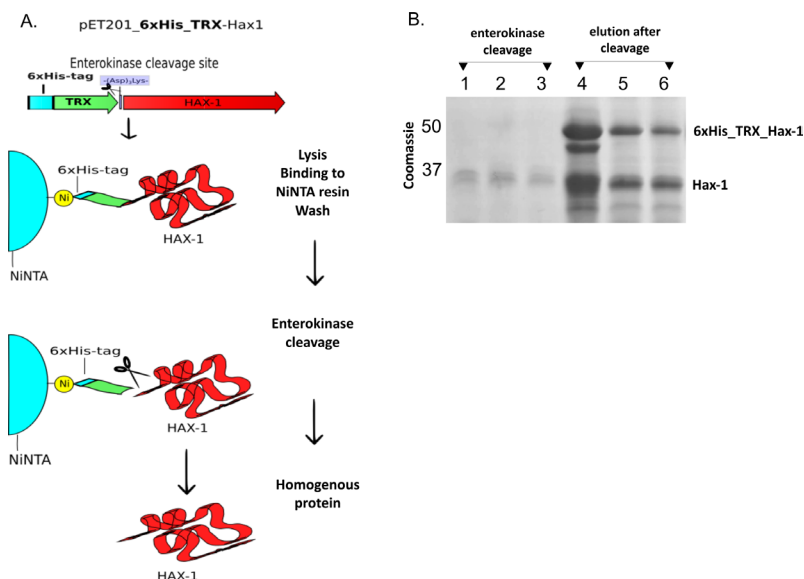


**Figure 2. Enterokinase cleavage and tags removal from the recombinant Hax-1 protein.**

(A) Schematic of tags' localization and cleavage for the pET201\_6xHis\_TRX\_Hax-1 construct. (B) Coomassie staining after enterokinase cleavage, lanes: 1-3. protein collected in digestion buffer, after "on-beads" enterokinase cleavage, no elution, 4-6. elution after cleavage, lanes 1 and 4: 4°C, 16 hours, lanes 2 and 5: 37°C, 12 hours; 3 and 6: 37°C, 16 hours.

### Structure prediction analysis

Secondary structure prediction for the rat and human Hax-1 demonstrates that the protein displays only a very few definite structural features, with two alpha helices flanking the protein ends, and short beta strands towards the C-terminal region of the protein (138-170 aa) (Supplementary Fig. 2 at [www.actabp.pl](http://www.actabp.pl)). A substantial part of the protein was predicted to be disordered. The PONDR (Predictor of Natural Disordered Regions) analysis of the Hax-1 sequence revealed that four disordered segments comprised about 41% of the protein, with the longest disordered segment of 31 aa present at the C-terminal region (152-182 aa) (Supplementary Fig. 3 at [www.actabp.pl](http://www.actabp.pl)).

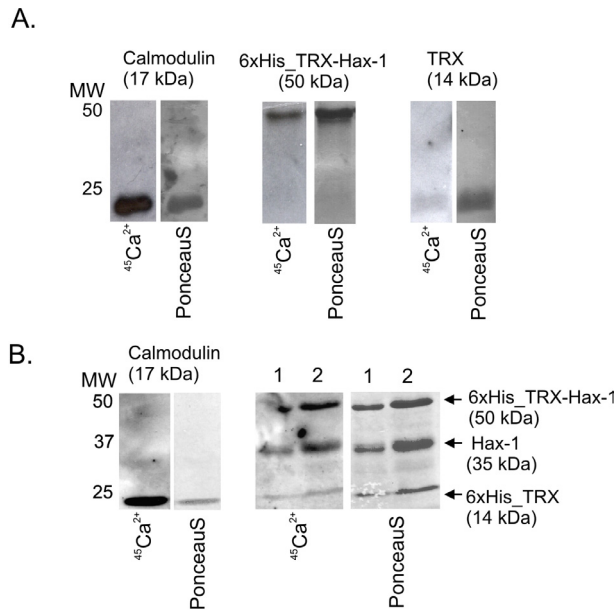


**Figure 3.**  $^{45}\text{Ca}^{2+}$  binding by recombinant and homogenous Hax-1. **(A)** Tagged, recombinant Hax-1,  $\text{Ca}^{2+}$  binding assay and PonceauS staining of the same membrane. Molecular weight marker: Precision Plus Protein Dual Color Standards, lanes: calmodulin (positive control) 4  $\mu\text{g}$ , 6xHis\_TRX\_Hax-1 extracted from the resin by boiling in 1.5 ml, loading volume: 45  $\mu\text{l}$ , TRX\_6xHis, loading volume: 45  $\mu\text{l}$  **(B)** Protein preparation after enterokinase cleavage (16 hours),  $\text{Ca}^{2+}$  binding assay and PonceauS staining of the same membrane. Lanes: calmodulin (positive control) 4  $\mu\text{g}$ , lanes 1 and 2: elution after enterokinase cleavage, three products: (1) 6xHis\_TRX-tagged Hax-1, 50 kDa (2) untagged Hax-1, 35 kDa (3) thioredoxin with His-tag, 14 kDa. Loading volume for lanes 1 and 2: 20, 40  $\mu\text{l}$ , respectively, estimated amount of Hax-1 protein, for lanes 1 and 2: upper band 3.5  $\mu\text{g}$ , 7  $\mu\text{g}$ , lower band: 3  $\mu\text{g}$ , 6  $\mu\text{g}$ , respectively.

Next, the sequence of the rat Hax-1 protein (278 aa; NCBI Acc. no. NP\_853658.1) was used as a query for the I-TASSER meta server. Secondary structure predictions of the protein made by this server are very roughly consistent with those generated by the PredictProtein 2013 algorithm. This analysis was followed by calculating five 3-dimensional models. The best model of Hax-1 had a C-score of  $-2.47$ . Typically, this parameter ranged from  $-5$  to  $2$ , and the higher value signifies models with higher confidence. The estimated accuracy of the model, measured by the TM-score, was  $0.43 \pm 0.14$ . A TM-score higher than  $0.5$  indicated that the model had the correct topology.

Predicting gene ontology (GO) revealed that Hax-1 may be a GTP-binding protein, and exhibits a GTPase activity (both GO-scores equalled  $0.62$ ). The GO-score is defined as the average weight of the GO-terms, where the weights were assigned based on the global and local similarities between the query and the template protein. Predictions with the GO-score  $> 0.5$  were treated as highly reliable. As to the ligand-binding capabilities of the protein, the calculations made by the I-TASSER meta server suggested that it was equally probable that Hax-1 binds to one of the following partners: N-acetyl-L-cysteine, peptides,  $\text{Zn}^{2+}$  or  $\text{Ca}^{2+}$ . All of these potential interactions had the same C-score of  $0.05$ . In Fig. 4, one can find the best 3-dimensional structure of rat Hax-1, generated by I-TASSER, with indicated six amino acids that may be involved in  $\text{Ca}^{2+}$  binding. Additionally, an animation of the same protein model is provided in the Supplement (Video 1 at [www.actabp.pl](http://www.actabp.pl)).

## DISCUSSION

The Hax-1 protein has been implicated in many cellular processes and protein-protein interactions, but knowledge about its structure and mechanisms of actions remains elusive. Efficient overexpression and purification of this protein should be the first step towards crystallization or other approaches to elucidate its structure and biophysical properties. Herein, we present a method for overexpression and purification of the untagged Hax-1 protein. This method is a modification of the previously described procedure, with the expression vector allowing for one-step tags' removal. The cleavage yielded very low amount of untagged protein. Instead, the elution yielded not only the untagged, tagged protein, but also the cleaved, untagged Hax-1. The plausible explanation could be that the cleaved product was not efficiently transferred to the digestion buffer. Thus, a mixture of the tagged and untagged Hax-1 protein was used in the autoradiography assay. Eluted proteins were separated in a polyacrylamide gel, so the recombinant protein with a large thioredoxin tag (50 kDa) could be easily distinguished from the untagged protein (35 kDa). Each form of the protein gave a relatively strong signal coming from bound  $^{45}\text{Ca}^{2+}$ . In a recent study, Hirasaka and coworkers (2016) reported the possibility of calcium-induced conformational change at the C-terminal part of Hax-1 (region of 211-280 aa). The authors suggested that Hax-1 has calcium binding capabilities, but no direct evidence was provided. As pointed out earlier (Results, Structure prediction analysis), the structure prediction for Hax-1 revealed only a few short segments of a possible well-defined structure, while a substantial portion of the protein was predicted to be unstructured and disordered. It is known that intrinsically disordered proteins (IDPs) may acquire a specific conformation upon binding to their targets (Dyson & Wright 2005). IDPs are especially numerous among signaling and cancer-associated proteins (Ganguly & Chen 2015; Uversky *et al.*, 2008). Accordingly, it seems plausible, that Hax-1 adopts a fixed three-dimensional structure upon binding of  $\text{Ca}^{2+}$ . Hax-1 conformational change upon binding to the target might also provide an explanation for its promiscuity in binding to many protein targets (Fadell & Grzybowska 2009), as was proven for other proteins, for example, the tumor suppressor protein TP53 (Wells *et al.*, 2008).

Due to the lack of homology and defined structural features, modeling of Hax-1 is quite challenging. Herein, we present a 3D model of the rat Hax-1 protein, computed by the I-TASSER meta server. This *in silico* analysis suggests that the C-terminus of Hax-1 contains a calcium-binding like motif, which is consistent with the findings by Hirasaka and coworkers (2016). Our results advocate that Hax-1 binds  $\text{Ca}^{2+}$  and that the C-terminal part of the protein might be involved in this binding.

## Acknowledgements

This work was supported by the Polish National Science Center grants no. 2011/01/B/NZ1/03674 and 2014/14/M/NZ1/00437.

## REFERENCES

- Al-Maghrebi M, Brule H, Padkina M, Allen C, Holmes WM, Zehner ZE (2002) The 3' untranslated region of human vimentin mRNA interacts with protein complexes containing eEF-1gamma and HAX-1. *Nucleic Acids Res* **30**: 5017–5028
- Chao JR, Parganas E, Boyd K, Hong CY, Opferman JT, Ihle JN (2008) Hax1-mediated processing of HtrA2 by Parl allows sur-

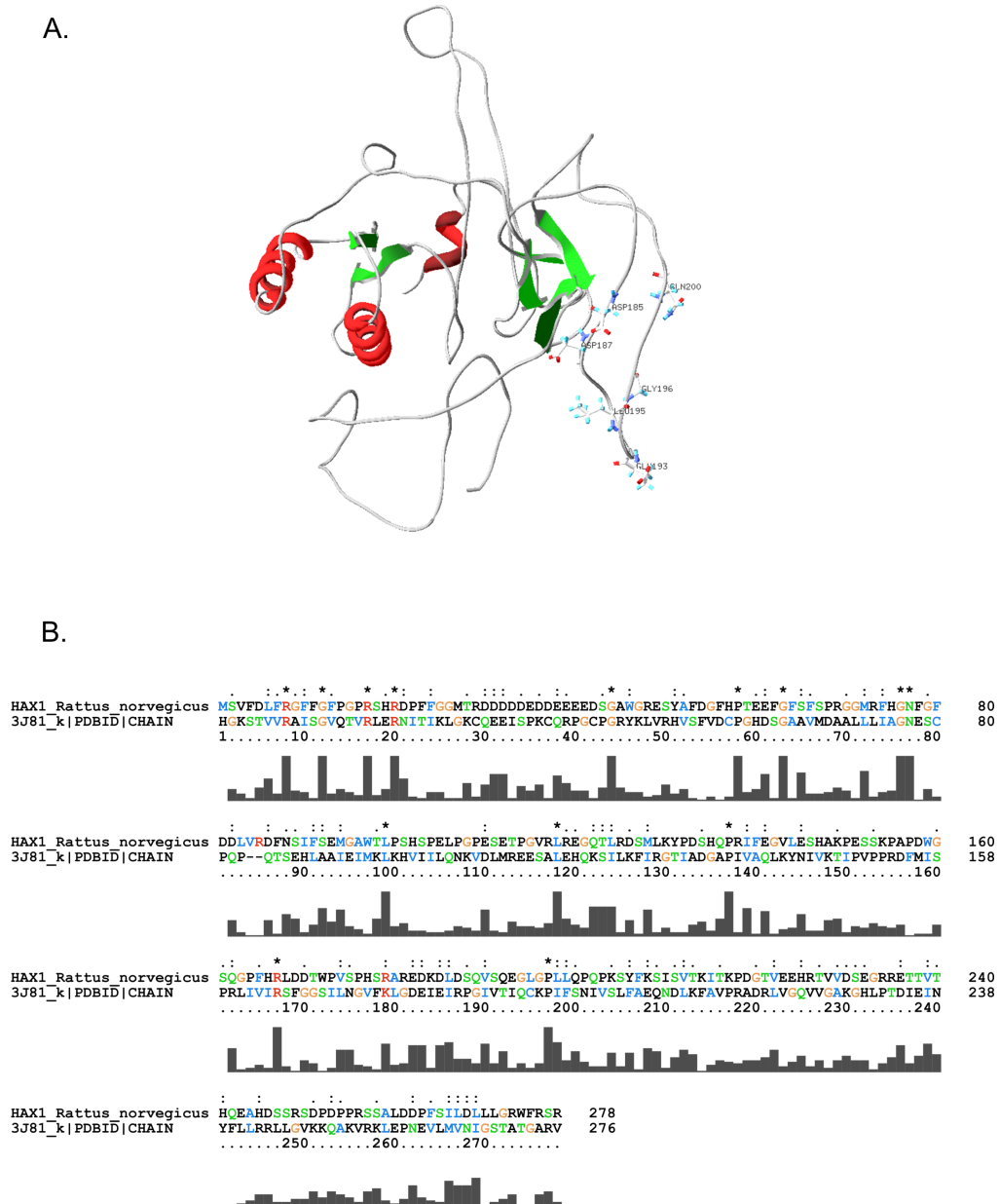


**Figure 4. Hax-1 model and sequence alignment generated by I-TASSER.**

(A) The best 3-dimensional structure of rat Hax-1. Alpha-helices are shown in red, beta strands in green. Amino acids predicted to be potentially involved in  $Ca^{2+}$  binding are marked with sticks. (B) Sequence alignment of the best analogue (Gcd11p, the gamma subunit of eIF2 translation initiation factor, PDB ID: 3J81) generated with Clustal X (v. 2.1). Alignment results: identity – 0.051, sequence coverage – 0.993, TM-score – 0.92, normalized Z-score of the threading alignments – 1.10. Stars denote identical residues, dots – residues with similar properties. Coloring scheme is based on the physical and chemical properties of amino acids.

- vival of lymphocytes and neurons. *Nature* **452**: 98–102. <http://doi.org/10.1038/nature06604>
- Cilenti L, Soundarapandian MM, Kyriazis GA, Stratico V, Singh S, Gupta S, Bonventre JV, Alnemri ES, Zervos AS (2004) Regulation of HAX-1 anti-apoptotic protein by Omi/HtrA2 protease during cell death. *J Biol Chem* **279**: 50295–50301. <http://doi.org/10.1074/jbc.M406006200>
- Dyson HJ, Wright PE (2005) Intrinsically unstructured proteins and their functions. *Nat Rev Mol Cell Biol* **6**: 197–208. <http://doi.org/10.1038/nrm1589>
- Fadeel B, Grzybowska E (2009) HAX-1: a multifunctional protein with emerging roles in human disease. *Biochim Biophys Acta* **1790**: 1139–1148. <http://doi.org/10.1016/j.bbagen.2009.06.004>
- Gallagher AR, Cedzich A, Gretz N, Somlo S, Witzgall R (2000) The polycystic kidney disease protein PKD2 interacts with Hax-1, a protein associated with the actin cytoskeleton. *Proc Natl Acad Sci U S A* **97**: 4017–4022
- Ganguly D, Chen J (2015) Modulation of the disordered conformational ensembles of the p53 transactivation domain by cancer-associated mutations. *PLoS Comput Biol* **11**: e1004247. <http://doi.org/10.1371/journal.pcbi.1004247>
- Han Y, Chen YS, Liu Z, Bodyak N, Rigor D, Bisping E, Pu WT, Kang PM (2006) Overexpression of HAX-1 protects cardiac myocytes from apoptosis through caspase-9 inhibition. *Circ Res* **99**: 415–423. <http://doi.org/10.1161/01.RES.0000237387.05259.a5>
- Hirasaka K, Mills EM, Haruna M, Bando A, Ikeda C, Abe T, Kohno S, Nowinski SM, Lago CU, Akagi K, Tochio H, Ohno A, Teshima-Kondo S, Okumura Y, Nikawa T (2016) UCP3 is associated with Hax-1 in mitochondria in the presence of calcium ion. *Biochem Biophys Res Commun* **472**: 108–113. <http://doi.org/10.1016/j.bbrc.2016.02.075>
- Jeyaraju DV, Cisbani G, De Brito OM, Koonin EV, Pellegrini L (2009) Hax1 lacks BH modules and is peripherally associated to heavy membranes: implications for Omi/HtrA2 and PARL activity in the regulation of mitochondrial stress and apoptosis. *Cell Death Differ* **16**: 1622–1629. <http://doi.org/10.1038/cdd.2009.110>
- Kang YJ, Jang M, Park YK, Kang S, Bae KH, Cho S, Lee CK, Park BC, Chi SW, Park SG (2010) Molecular interaction between HAX-1

- and XIAP inhibits apoptosis. *Biochem Biophys Res Commun* **393**: 794–799. <http://doi.org/10.1016/j.bbrc.2010.02.084>
- Klein C, Grudzien M, Appaswamy G, Germeshausen M, Sandrock I, Schaffer AA, Rathinam C, Boztug K, Schwitzer B, Rezaei N, Bohn G, Melin M, Carlsson G, Fadeel B, Dahl N, Palmblad J, Henter JI, Zeidler C, Grimbacher B, Welte K (2007) HAX1 deficiency causes autosomal recessive severe congenital neutropenia (Kostmann disease). *Nat Genet* **39**: 86–92. <http://doi.org/10.1038/ng1940>
- Kokoszynska K, Rychlewski L, Wyrwicz LS (2010) Distant homologs of anti-apoptotic factor HAX1 encode parvalbumin-like calcium binding proteins. *BMC Res Notes* **3**: 197. <http://doi.org/10.1186/1756-0500-3-197>
- Li B, Hu Q, Xu R, Ren H, Fei E, Chen D, Wang G (2012) Hax-1 is rapidly degraded by the proteasome dependent on its PEST sequence. *BMC Cell Biol* **13**: 20. <http://doi.org/10.1186/1471-2121-13-20>
- Maruyama K, Mikawa T, Ebashi S (1984) Detection of calcium binding proteins by <sup>45</sup>Ca autoradiography on nitrocellulose membrane after sodium dodecyl sulfate gel electrophoresis. *J Biochem* **95**: 511–519
- Radhika V, Onesime D, Ha JH, Dhanasekaran N (2004) Galpha13 stimulates cell migration through cactactin-interacting protein Hax-1. *J Biol Chem* **279**: 49406–49413. <http://doi.org/10.1074/jbc.M408836200>
- Ramsay AG, Keppler MD, Jazayeri M, Thomas GJ, Parsons M, Viollette S, Weinreb P, Hart IR, Marshall JF (2007) HS1-associated protein X-1 regulates carcinoma cell migration and invasion via clathrin-mediated endocytosis of integrin alphavbeta6. *Cancer Res* **67**: 5275–5284. <http://doi.org/10.1158/0008-5472.CAN-07-0318>
- Roy A, Kucukural A, Zhang Y (2010) I-TASSER: a unified platform for automated protein structure and function prediction. *Nat Protoc* **5**: 725–738. <http://doi.org/10.1038/nprot.2010.5>
- Sarnowska E, Grzybowska EA, Sobczak K, Konopinski R, Wilczynska A, Szwarc M, Sarnowski TJ, Krzyzosiak WJ, Siedlecki JA (2007) Hairpin structure within the 3'UTR of DNA polymerase beta mRNA acts as a post-transcriptional regulatory element and interacts with Hax-1. *Nucleic Acids Res* **35**: 5499–5510. <http://doi.org/10.1093/nar/gkm502>
- Suzuki Y, Demoliere C, Kitamura D, Takeshita H, Deuschle U & Watanabe T (1997) HAX-1, a novel intracellular protein, localized on mitochondria, directly associates with HS1, a substrate of Src family tyrosine kinases. *J Immunol* **158**, 2736–2744
- Trebinska A, Högstrand K, Grandien A, Grzybowska EA, Fadeel B (2014) Exploring the anti-apoptotic role of HAX-1 versus BCL-X<sub>L</sub> in cytokine-dependent bone marrow-derived cells from mice. *FEBS Lett* **588**: 2921–2927. <http://dx.doi.org/10.1016/j.febslet.2014.05.042>
- Trebinska A, Rembiszewska A, Ciosek K, Ptaszynski K, Rowinski S, Kupryjanczyk J, Siedlecki JA, Grzybowska EA (2010) HAX-1 over-expression, splicing and cellular localization in tumors. *BMC Cancer* **10**: 76. <http://doi.org/10.1186/1471-2407-10-76>
- Uversky VN, Oldfield CJ & Dunker AK (2008) Intrinsically disordered proteins in human diseases: introducing the D2 concept. *Annu Rev Biophys* **37**, 215–246. <http://doi.org/10.1146/annurev-biophys.37.032807.125924>
- Vafiadaki E, Arvanitis DA, Pagakis SN, Papalouka V, Sanoudou D, Kontrogianni-Konstantopoulos A, Kranias EG (2009) The anti-apoptotic protein HAX-1 interacts with SERCA2 and regulates its protein levels to promote cell survival. *Mol Biol Cell* **20**: 306–318. <http://doi.org/10.1091/mbc.E08-06-0587>
- Vafiadaki E, Sanoudou D, Arvanitis DA, Catino DH, Kranias EG, Kontrogianni-Konstantopoulos A (2007) Phospholamban interacts with HAX-1, a mitochondrial protein with anti-apoptotic function. *J Mol Biol* **367**: 65–79. <http://doi.org/10.1016/j.jmb.2006.10.057>
- Wells M, Tidow H, Rutherford TJ, Markwick P, Jensen MR, Mylonas E, Svergun DI, Blackledge M, Fersht AR (2008) Structure of tumor suppressor p53 and its intrinsically disordered N-terminal transactivation domain. *Proc Natl Acad Sci U S A* **105**: 5762–5767. <http://doi.org/10.1073/pnas.0801353105>
- Yachdav G, Kloppmann E, Kajan L, Hecht M, Goldberg T, Hamp T, Honigschmid P, Schafferhans A, Roos M, Bernhofer M, Richter L, Ashkenazy H, Punta M, Schlessinger A, Bromberg Y, Schneider R, Vriend G, Sander C, Ben-Tal N, Rost B (2014) PredictProtein—an open resource for online prediction of protein structural and functional features. *Nucleic Acids Res* **42**: W337–W343. <http://doi.org/10.1093/nar/gku366>
- Yang J, Yan R, Roy A, Xu D, Poisson J, Zhang Y (2015) The I-TASSER Suite: protein structure and function prediction. *Nat Methods* **12**: 7–8. <http://doi.org/10.1038/nmeth.3213>
- Zhang Y (2008) I-TASSER server for protein 3D structure prediction. *BMC Bioinformatics* **9**: 40. <http://doi.org/10.1186/1471-2105-9-40>